Atmospheric
Chemistry
and Physics
Discussions

Open Access

Climatology of new particle formation events in the subtropical North Atlantic free troposphere at Izaňa GAW observatory

M. I. García[1,2], S. Rodríguez[1], Y. González[1], and R. D. García[1,3]

[1]Izaña Atmospheric Research Centre, AEMET, Associated Unit to CSIC "Studies on Atmospheric Pollution", La Marina 20, Planta 6, E38071, Santa Cruz de Tenerife, Canary Islands, Spain
[2]Department of Analytical Chemistry, Nutrition and Food Science, University of La Laguna, Avda. Astrofísico Fco. Sánchez s/n, 38200, La Laguna, Tenerife, Canary Islands, Spain
[3]Atmospheric Optic Group, University of Valladolid (GOA, UVA), Prado de la Magdalena s/n, 47071, Valladolid, Spain

Correspondence to: M. I. García (isabel_garciaalvarez@hotmail.es)

Discussion Paper | Discussion Paper | Discussion Paper | Discussion Paper |

ACPD

13, 24127–24169, 2013

Climatology of new particle formation events at Izaña GAW observatory

M. I. García et al.

Title Page

Abstract | Introduction

Conclusions | References

Tables | Figures

◄ | ►

◄ | ►

Back | Close

Full Screen / Esc

Printer-friendly Version

Interactive Discussion

Abstract

A climatology of new particle formation (NPF) events in the subtropical North Atlantic free troposphere is presented. A four year data set (June 2008–June 2012), which includes number size distributions (10–600 nm), reactive gases (SO_2, NO_x, and O_3), several components of solar radiation and meteorological parameters, measured at Izaña Global Atmospheric Watch observatory (2400 m above sea level; Tenerife, Canary Islands) was analysed. On average, NPF occurred during 30 % of the days, the mean values of the formation and growth rates during the study period were 0.49 $cm^{-3} s^{-1}$ and 0.42 $nm\,h^{-1}$, correspondingly. There is a clearly marked NPF season (May to August), when these events account for 50 to 60 % of the days/month. Monthly mean values of the formation and growth rates exhibit higher values during this season (0.50–0.95 $cm^{-3} s^{-1}$ and 0.48–0.58 $nm\,h^{-1}$, respectively) than during other periods. The two steps (formation and growth) of the NPF process mostly occur under the prevailing northern winds typical of this region. Sulphur dioxide and UV radiation show higher levels during NPF events than in other type of episodes. The presence of Saharan dust in the free troposphere is associated with a decrease in the formation rates of new particles. In the analysis of the year-to-year variability, mean sulphur dioxide concentration (within the range 60–300 ppt) was the parameter that exhibited the highest correlation with the frequency of NPF episodes. The availability of this trace gas (i.e. their oxidation products) seems also to have a influence on the duration of the events, number of formed nucleation particles, formation rates and growth rates. We identified a set of NPF events in which two nucleation modes (that may evolve at different rates) occur simultaneously and for which further investigations are necessary.

1 Introduction

The growth of nucleated molecules is an important source of atmospheric aerosols (Kulmala, 2003). It is considered that the so-called "new particle formation" (NPF) is a

two step (decoupled) process: nucleation and growth. It has been proposed that the nucleation of sulphuric acid gas molecules results in the formation of stable clusters (>2 nm size; Kulmala et al., 2006; Kulmala and Kerminen , 2008). Under certain scenarios these clusters are "activated" in such a way that they growth up to result in stable aerosols with a size $\geq$ 50 nm (e.g. during the so-called "banana type growth" events). Processes involved in the NPF (nucleation and growth up to stable sizes) are not fully understood. For the first phase, or nucleation, the most studied mechanisms are binary (water - sulphuric acid), ternary (water – sulphuric acid – ammonia) and ion – induced nucleation (see the Kulmala, 2003 discussion). For the second phase, or growth, the proposed mechanisms include condensation of sulphuric acid – sulphate and organic vapours (Laaksonen et al., 2008).

Understanding how nucleated clusters and particles growth is important for studying the influence of aerosols on climate, including feedbacks (IPCC, 2007). This influence depends on particle size. Nucleation not followed by growth processes (e.g., bursts, also so-called "apple" type events) typically results in high concentrations of particles < 20 nm size. These particles have a short lifetime (∼ hours), have a low ability to act as cloud condensation nuclei (McFiggans et al., 2006) and exhibit Rayleigh scattering features (as gases). In contrast, accumulation mode particles (100–1000 nm) are long lived (∼ few weeks), are good condensation nuclei and scatter light more efficiently. Because of the influence of thermodynamic processes (e.g. T and RH), UV radiation and meteorology on the NPF processes, climate may also affect NPF. Emission rates of gaseous precursors also play a key role. The decadal decrease (2001–2010) in the total particle number concentration (a metric dominated by particles < 20 nm) observed at background and remote sites in Europe, North America and the Pacific has been attributed to a decrease of anthropogenic emissions of gaseous precursors (Asmi et al., 2012).

Long term studies ($\geq$ 1 yr) on NPF, which include the determination of the new particle formation rate (FR) and growth rate (GR), at mountain sites that reach the free troposphere are scarce (Fig. 1; see also Kulmala et al., 2004). These long term studies

Climatology of new particle formation events at Izaña GAW observatory

M. I. García et al.

Title Page

Abstract	Introduction
Conclusions	References
Tables	Figures

|◄ | ►|
◄ | ►

Back | Close

Full Screen / Esc

Printer-friendly Version

Interactive Discussion

Climatology of new
particle formation
events at Izaña GAW
observatory

M. I. García et al.

Title Page

Abstract | Introduction

Conclusions | References

Tables | Figures

◀ | ▶

◀ | ▶

Back | Close

Full Screen / Esc

Printer-friendly Version

Interactive Discussion

have mostly been performed in the continental boundary layer (e.g. Birmili et al., 2000; Dal Maso et al., 2005; Hamed et al., 2007). Studies of NPF at mountain sites are of interest for several reasons. Because mountain upslope winds are frequently linked to high ultrafine particle concentrations (Weber et al., 1995; Venzac et al., 2008), elevated mounts may act as source regions for new particles in the free troposphere (FT), where these 'grown particles' may experience long range transport due to the much higher wind speeds than in the boundary layer and may act as cloud condensation nuclei (CCN).

The objective of this work is to study NPF events in the North Atlantic free troposphere at the Izaña mountain observatory. In this study, based on 4 yr data, the frequency of NPF events, formation rates and growth rates were determined; the processes that influence NPF and the formation and growth rates were studied. Results obtained at Izaña were compared with those obtained at other observatories.

2 Methodology

2.1 Study area

Izaña Global Atmospheric Watch (GAW) observatory (16°29′58″ W; 29°18′32″ N) is located in Tenerife island, at 2367 m a.s.l (Fig. 1a). The observatory (Fig. 1b) remains almost permanently in the low free troposphere, i.e. above the marine stratocumulus layer typical of the subtropical oceans. NW dry subsiding airflows dominate throughout the year except in summer, when they are frequently alternated with SE airflows from North Africa. Below the stratocumulus layer, the humid and cool NNE trade winds dominate. The development of orographic thermal-buoyant upward flows during daylight results in the upward transport of water vapour and trace gases emitted at low altitudes by biogenic and anthropogenic sources (see details in Rodríguez et al., 2009).

2.2 Measurements

This study is based on a 4 yr data set (June 2008 to June 2012) of particle size distributions (10–600 nm), reactive gases (SO_2, NO_x, O_3), meteorological parameters (temperature, humidity, water vapour, wind speed, wind direction) and radiation (global, direct, diffuse, UV-B, UV-A).

2.2.1 Particle Size Distribution

Particle size distribution within the range 10–600 nm was measured with a TSI™ Scanning Mobility Particle Sizer (SMPS, model 3996). Two different Condensation Particle Counters (CPCs) were used as detectors: a CPC-3025A, from June 2008 to March 2009, and a CPC-3010 from March 2009 on. These instruments have been subjected to several quality assurance and quality control activities. The 50 % efficiency diameters (Dp_{50}) were determined in the World Calibration Centre for Aerosol Physics (WCCAP, Institute for Tropospheric Research, Leipzig, Germany): 2.4 nm for the CPC-3025A unit (SN: 1160; Sept 2002 and 9.6 nm for the CPC-3010 unit (SN: 70431239; Sept 2011). The SMPS was intercompared, measuring ambient air aerosol, with similar TSI™ – SMPS instruments in April 2010 and November 2012 within the REDMAAS network (www.redmaas.com; Gómez-Moreno et al., 2013). In these exercises the sizing accuracy was also assessed with monodisperse poly-styrene latex spheres of 80 and 190 nm, a discrepancy of -1% and -1.2% was found, respectively. During the regular operations at Izaña, the SMPS is subject to weekly checks of "aerosol and sheath airflows", zeroes and leak tests using absolute filters.

At Izaña, the aerosol instrumentation (SMPS and other devices) are located in a 6 m high building so-called "PARTILAB" (particles laboratory; Fig. 1b), where the indoor temperature is set to 20 °C. Temperature, relative humidity (RH) and pressure are monitored in the aerosol flow (stretch of sampling pipe into the building, just before the aerosol monitors) and in the outdoor ambient air. Temperature and RH in the aerosol flow and in the outdoor ambient air is shown in Fig. 2. Outdoor ambient RH is

usually low (70th percentile is $\sim 40\,\%$ for hourly annual data). Because of the higher indoor temperature, the RH in the sample is usually much lower, within the range 10 to 25 % (25th–75th percentiles for annual hourly data). Thus, dry aerosol measurements are performed without using any system for reducing RH (membrane/nafion driers, or dilutors).

The SMPS data availability is 74 % for the study period (June 2008–June 2012). Non-valid data were flagged and not analysed. Subsequently, data were normalized to 1013.25 hPa and 273.15 K. Correction for diffusion losses in the sampling pipe and inside the SMPS were applied (Hinds, 1999).

2.2.2 Reactive gases and dust

Reactive gases were measured using different principle of measurements: UV fluorescence analyser for SO_2 (Thermo™, model 43C-TL), UV absorption for O_3 (Thermo™, model 49C) and chemiluminescence for NO, NO_2 and NO_x (Thermo™, model 42C-TL). In order to avoid the NO_2 overestimation linked to the use of molybdenum converters, a photolytic NO_2 to NO converter was used (Parrish and Fehsenfeld , 2000; Steinbacher et al., 2007). Quality Assurance and Quality Control activities included: (i) 15 min zero measurements, performed every 24-h in the SO_2 and O_3 and every 6-h in the NO_x analysers, (ii) the use of linear fittings between consecutive zeros for applying zero correction to data, (iii) 5-points span calibrations every 3 months with certified SO_2 and NO_x concentrations, and (iv) calibration of the O_3 analyser versus an O_3 primary standard (49C – PS). A high linearity was commonly observed in these calibrations ($r^2 \sim 0.999$). Detection limit is 60 ppt for SO_2, 50 ppt for NO and NO_x (5-min average) and 1 ppb for O_3 (1-min average).

Dust concentrations were measured by combining two techniques: sampling on filter for further chemical characterisation and using an Aerodynamic Particle Sizer (see details in Rodríguez et al., 2011).

Title Page

Abstract | Introduction

Conclusions | References

Tables | Figures

◄ | ►

◄ | ►

Back | Close

Full Screen / Esc

Printer-friendly Version

Interactive Discussion

2.2.3 Radiation

The Izaña observatory is part of the Baseline Surface Radiation Network (BSRN) since 2009 (García, 2011). We used shortwave downward radiation (SDR) irradiance (global, direct and diffuse), UV-A and UVB measurements. The global and diffuse SDR were measured with unshaded and shaded Kipp and Zonen CM-21 pyranometers, respectively. The spectral range covers 335 to 2200 nm (95 % points) and the expected uncertainty is ±2 % for hourly totals. The direct SDR is measured with a Kipp and Zonen CH1 pyrheliometer, with a field of view limited to $5° ± 0.2°$, placed on a Sun Tracker with a tracking accuracy of $0.1°$. The spectral range goes from 200 to 4000 nm (50 % points) and the uncertainty of this measurement is ±2 % for hourly totals. The UV-A is measured with Kipp and Zonen UVS-A-T radiometer. The spectral range covers 315 to 400 nm with daily uncertainty lower than 5 %. The UV-B is measured with Yankee Environmental System (YES) UVB-1 pyranometer. The spectral range goes from 280 to 320 nm. All radiation parameters are measured with 1-min resolution.

2.2.4 Meteorology

Meteorological parameters were measured using a Setra 470 instrument for pressure, a Rotronic for temperature and relative humidity, and a Thies Sonic anemometer for wind. Concentrations of water vapour were calculated with the Magnus equation. Vertical wind only was recorded from June 2011 to October 2011.

2.3 Characterization of NPF Events

2.3.1 Classification of events

Plots with "5 min time resolution 3-D – dN/dlog" data for each day were visually analysed for identifying the "banana type" NPF events (Dal Maso et al., 2005). Seven types of events were considered (Table 1 and Fig. 3). In events class I and II a clear particle formation and growth was observed during at least 4 and 2 h, respectively. In class

III events no particle growth was observed after the particle burst (Apple type events; Yli-Juuti et al., 2009). The remaining events were sorted as: No Event (no increase in the concentration of particles < 25 nm was observed), Undefined (event was not clearly observed) or Bad data (invalid or missing data).

2.3.2 Determination of formation and growth rates

We attempted to determine the FR and GR for all class I events. However, this was not possible for set episodes in which a noisy signal was observed, mostly induced by a significant variability in the horizontal and/or vertical components of wind. Thus, events in which the FR and GR could be determined were sub-classified as class Ia, the remaining events were labelled as class Ib (Table 1).

The FR (J_D) and GR were calculated for the nucleation mode particles (Dp < 25 nm) using the approximation for relatively clean and homogenous air masses of Kulmala et al., 2004:

$$J_D \approx \frac{\Delta N_{Dp,Dp_{max}}}{\Delta t} \tag{1}$$

where $\Delta N_{Dp,Dp_{max}}$ is the total particle number concentration in the size range [Dp, Dp_{max}] and Dp_{max} is the maximum size that the critical clusters may reach because of their growth during Δt. J_D is the slope obtained from the first-order polynomial fitting during the episode when representing the nucleation mode particle concentration as a function of time (Fig. 4). Similarly:

$$GR \approx \frac{\Delta Dp_m}{\Delta t} \tag{2}$$

where Dp_m belongs to the size range [Dp, Dp_{max}]. GR is the slope obtained from the first-order polynomial fitting during the episode when representing the nucleation mode geometric mean diameter as a function of time (Fig. 4). The FR and GR were determined using Eqs. (1) and (2) in two different approaches.

Method 1: SMPS data

The FR and GR were determined for the nucleation mode particles (Dp < 25 nm) using the number concentration (N_{nuc}; Dal Maso et al., 2005) and the geometric mean diameter (GMD, Dp$_{nuc}$; Järvinen et al., 2013) of the 5 min resolution SMPS data. We used the GMD to avoid the human bias associated with other methods such as visual determination of the mode size change. Figure 4b shows an illustration of the linear fittings used for determining the slopes FR (Eq. 1) and GR (Eq. 2). Results are shown in Figs. 7–9 (discussed below).

Method 2: lognormal size distribution

This method was implemented in two steps. First, each 5 min average size distribution was fitted to a linear combination of lognormal distributions:

$$\frac{dN}{d\ln D_p} = \Sigma^n_{(i=1)} \frac{N_i}{\sqrt{2\pi \ln \sigma_{(g,i)}}} \exp(-\frac{(\ln D_p - \ln D_{p(g,i)})^2}{2\ln^2 \sigma_{(g,i)}}) \tag{3}$$

Each lognormal distribution is characterized by three parameters: mean number concentration N_i, geometric variance $\sigma^2_{g,i}$ and the geometric mean diameter $D_{p(g,i)}$. The fitting procedure was performed in a script programmed in Matlab™. The fitting accuracy was assessed by the Least Squares Quadratic (LSQ) value between the measured particle number size distribution and its fitting. This method is usually applied considering a single nucleation mode (< 25 nm), e.g. by Boy et al. (2008); Dal Maso et al. (2005); Salma et al. (2011); Yli-Juuti et al. (2009). However, we observed that in many cases, the LSQ value was significantly reduced if the nucleation mode was fitted with 2 lognormal fittings instead of 1. In many cases a simple visual analysis of the 5 min size distributions evidenced that the nucleation mode growth was prompted by one of these

lognormal distribution. Results are shown in Fig. 12 (discussed below). In the second step, FR and GR were determined using Eqs. (1) and (2).

3   Results and discussion

3.1   Upward transport of particle precursors

The daily evolution (hourly mean values throughout the day) of the particle size distribution, particle concentration and geometric mean diameter of the nucleation mode, SO_2, NO_x, UV-B radiation and some meteorological parameters, averaged for each season is shown in Fig. 5. At Izaña, the number of particles exhibits strongly marked daily cycles, with much higher values during daylight than at night (Fig. 5b). This daylight increase is associated with a parallel increment in the RH and in the concentrations of SO_2, NO_x and RH, which is prompted by the arrival of air from lower altitudes due to the development of orographic buoyant upward flows. The influence of these upward airflows on the concentrations of precursors and nanoparticles (< 10 nm) at Izaña mount was described in detail by Rodríguez et al. (2009). These upward airflows carrying precursors and other gaseous pollutants from the boundary layer were also observed in other mountain observatories located in islands, such as Pico in Azores (Kleissl et al., 2007) and Mauna Loa in Hawaii (Weber et al., 1995, 1999). This ascent of air masses tends to occur during daylight linked to the heating of the terrain (Fig. 5F3 and F4). Previous studies at Mauna Loa and Izaña concluded that NPF is favoured in the boundary layer to the free troposphere transition region due to the low surface area of pre-existing particles (prompted by in-cloud particle scavenging), the high solar radiation conditions above the marine cloud layer and the gaseous precursor supply by the upward flows.

The high frequency of NPF events at Izaña results in a strongly marked daily cycle in the mean particle size distributions (Fig. 5a and b): after the increase in the number of particles < 25 nm (hereinafter so-called nucleation particles, N_{nuc}) typically observed between 10:00 and 12:00 GMT (depending on the season), a progressive increase in

the geometric mean diameter is observed, in some cases even until the evening. These observations indicate that formation and growth of new particles > 10 nm tend to occur during the daylight upward flow period. This evidences that the nanoparticles (< 10 nm) observed by Rodríguez et al. (2009) at Izaña frequently grow up to reach higher and stable diameters.

3.2 Classification of episodes

A total of 1178 days were classified in the study period (June 2008–June 2012). The distribution of these events among the seven considered categories is shown in Table 2. Figure 6 shows the monthly distribution of episodes. Events in which a burst of nucleation particles (< 25 nm) followed by particle growth (banana events) was observed during at least 2 h (type Ia + Ib + II; examples in Fig. 3) accounted for ∼ 30 % of the 4 yr observations. Events with a duration longer than 4 h (I = Ia + Ib) accounted for ∼ 11 % of the days. These banana events (I + II) mostly occurred from May to October, when they accounted for more than 30 % of the days of each month (Fig. 6a). The frequency of these events was at a maximum from June to August, when they accounted for 50 to 60 % of the days/month (Fig. 6a). In these months, 50 to 75 events per month were observed during the 4 study years (Fig. 6b).

Events type III (burst of nucleation particles not followed by particle growth, also so-called apple type events) occurred throughout the year, with a frequency within the range 5–12 %, without any significant seasonal behaviour (Fig. 6c). This indicates that although the formation of nucleation particles occurs throughout the different seasons (Fig. 6c), conditions for the particle growth mostly occur from May to October (Fig. 6a and b). Undefined events showed a higher frequency in July–August (Fig. 6d), whereas no events mostly occurred from November to March (Fig. 6d).

The percentage of event days (I + II) we observed (∼ 30 %; Table 2) is somewhat lower than that observed at 5079 m a.s.l. in the Nepal Himalayas (∼ 43 %; Venzac et al., 2008) and in Puy de Dôme (∼ 38 %; Manninen et al., 2010), but higher than those observed at 2180 m a.s.l. in the Indian Himalayas (∼ 11 %; Neitola et al., 2011) and at

3580 m a.s.l. in the Swiss Alps ($\sim 20\%$; Jungfraujoch; Boulon et al., 2010; Manninen et al., 2010).

At Izaña FT site, the NPF season occurs from May to August, when events (I+II) occur with a frequency of $\sim 50\%$ (Fig. 6a). At Jungfraujoch (also FT) these events occur from the end of Spring to early Autumn ($\sim 25\%$ frequency during the season) as well, linked to the transport of precursors from the boundary layer (Boulon et al., 2010; Manninen et al., 2010). In the European continental boundary layer these events are mostly observed in Spring (Dal Maso et al., 2005; Hamed et al., 2007; Manninen et al., 2010), although in NW Italy they were mostly observed in Autumn linked to specific North-Foëhn meteorological conditions (Rodríguez et al., 2005). In Puy de Dôme mount, they have been observed in Spring and Autumn ($\sim 50\%$) probably because this site is within the boundary layer more frequently than other mountain observatories (Manninen et al., 2010). In the Nepal Himalayas these events were observed in the monsoon (July–September) and post-monsoon (October–December) seasons ($\sim 50\%$), whereas in the Indian Himalayas they occur in Spring ($\sim 80\%$ from March to June; Neitola et al., 2011. Järvinen et al. (2013) have reported these events taking place more often during the Antarctic summer.

3.3 Formation and growth rates of new particles

Figure 7 shows the monthly averages of the Formation Rates (FR), Growth Rates (GR) and other parameters during NPF events at Izaña from June 2008 to June 2012. As already described above, the FR and GR of the nucleation particles (< 25 nm) could only be calculated for a set of events class I, that were labelled as class Ia. These determinations were performed for a total of 109 Ia events using the method 1 described in section 2.3.2. At Izaña, NPF class Ia events: (a) exhibit higher monthly averaged FR from March to October (0.50–$0.95\,\mathrm{cm}^{-3}\,\mathrm{s}^{-1}$) than from April to September (0.20–$0.36\,\mathrm{cm}^{-3}\,\mathrm{s}^{-1}$; Fig. 7a). (b) Show slightly higher GR from April to July (0.48 to $0.58\,\mathrm{nm}\,\mathrm{h}^{-1}$) than from August to March (0.26–$0.44\,\mathrm{nm}\,\mathrm{h}^{-1}$; Fig. 7b). (c) Are longer from April to October (6 to 7 h) than from November to March (5–6 h; Fig. 7c). This

Climatology of new particle formation events at Izaña GAW observatory

M. I. García et al.

shift in the duration is also associated with a shift in the starting and ending time of the events, clearly linked with the seasonal shift in the daylight length (Fig. 7d).

Mean values of FR and GR at Izaña were compared with those observed at other mountain sites (Table 3). Unfortunately, because of the lack of long term studies, just mean values (and not seasonal behaviour) could be compared in most of the cases. GR at Izaña and Mauna Loa (both free troposphere sites in subtropical islands) are quite similar ($\sim 0.4\,\mathrm{nm\,h^{-1}}$). These are significantly lower than those observed in mountains located in continental regions (2–$15\,\mathrm{nm\,h^{-1}}$), where the higher regional emission of gaseous precursors and the enhanced vertical transport over the continental platform may account for the significantly higher GRs. FR at Izaña and Mauna Loa are also similar, however the low number of reported observations at mountain sites do not allow to reach any conclusion about differences between oceanic islands and continental regions. The amplitude of the seasonal variation of the FR at Izaña (min: $0.20\,\mathrm{cm^{-3}\,s^{-1}}$; max: $0.95\,\mathrm{cm^{-3}\,s^{-1}}$) is higher than that observed at Pyramid – Himalayas (min: $0.14\,\mathrm{cm^{-3}\,s^{-1}}$; max: $0.20\,\mathrm{cm^{-3}\,s^{-1}}$; Venzac et al., 2008), with max-GR to min-GR ratios equal to 4.7 at Izaña and 1.4 at Pyramid – Himalayas.

3.4 Context during NPF events

3.4.1 Type Ia events

In order to identify the parameters that influence the NPF a set of analyses were performed. Mean values of the gaseous pollutants (SO_2, NO_x and O_3), dust concentrations, radiation components (global, diffuse, direct, UV-A and UV-B) and meteorological parameters (T, RH, water vapour, wind vector components, speed and direction) were determined during the two steps of each NPF episode: (1) step-1 "formation of the nucleation particles" and (2) step-2 "subsequent particle growth". These determinations were performed for the 109 events of type Ia. The resulting data base was then subjected to different analysis (Tables 4 and 5; Figs. 8–11).

Table 4 shows the ratios of the mean value of each parameter during the formation (F) and growth (G) steps to the average value at Izaña. The same parameters show high ratios (> 1.5) during the formation and during the growth steps: sulphur dioxide (ratios 2.3–2.2), vertical wind component (1.8–2.2), UV-B (1.9–1.8), global (1.6–1.5) and UV-A (1.6–1.5) radiation. This supports the idea that upward transport of sulphur dioxide (from the boundary layer) and its further photo-oxidation by UV radiation is a key process in the NPF. The low wind speed ratios observed during the formation and growth steps (≤ 0.6) indicate that these events occur under low synoptic wind speed conditions.

Mean values of the study parameters during the formation and growth steps were plotted against wind direction (Fig. 8). Most of the formation step and growth step events occur under northern (N–NNE) wind conditions ($\sim 50\%$ for the F and 27 % for G steps, respectively) and secondarily under eastern (ENE–E) and western (WNW–W) winds ($\sim 10\%$ for both directions; Fig. 8A2 and B2). Formation and growth rates exhibit a significant variability with wind direction (Fig. 8A2 and B2): (a) FR under the predominant northern winds conditions are about twice ($\sim 0.6\,\mathrm{cm}^{-3}\,\mathrm{s}^{-1}$) those observed from the East and West directions ($\sim 0.35\,\mathrm{cm}^{-3}\,\mathrm{s}^{-1}$); (b) GR recorded under eastern winds ($0.6\,\mathrm{nm}\,\mathrm{h}^{-1}$) are higher than those observed from the North and West (0.35 to $0.40\,\mathrm{nm}\,\mathrm{h}^{-1}$).

The highest FR and GR are observed when air blows from the eastern side (0–180°). This sector is also associated with the highest SO_2 concentrations (Fig. 8A3 and B3). This precursor also influences the number of nucleation particles formed during the formation step (ΔN_{nuc}), the highest concentrations are recorded during NE winds (Fig. 8A4).

The data set of the type Ia events was also subjected to cross correlation analysis. Some interesting observations are (Fig. 9): (a) FR and GR do not show a high linear relationship (linear correlation) with SO_2, even if this is considered a key precursor (Fig. 9A1 and B1). This is attributed to the involvement of the SO_2 photo-oxidation, a process that results in the gas phase sulphuric acid and whose concentrations have

Climatology of new particle formation events at Izaña GAW observatory

M. I. García et al.

been observed to correlate with the concentrations of nanoparticles (Fiedler et al., 2005). In our analysis neither did we observe a linear relationship with the $SO_2 \cdot UV$ product, which suggests that other species, such as organic compounds, may be involved (Laaksonen et al., 2008). (b) FR is negatively correlated with wind speed (Fig. 9A1). This evidences how dilution of the gas phase precursors (by winds) makes it difficult to reach the saturation conditions necessary for the change of phase. Observe that $FR > 1.2\,cm^{-3}\,s^{-1}$ are observed when wind speed is $\leq 3.5\,m\,s^{-1}$. The anti-correlation of GR and wind speed seems to be weaker (Fig. 9B1). (c) FR is negatively correlated with Saharan dust (Fig. 9A3). This is attributed to the decrease in the gas phase concentration due to the reaction of SO_2/sulphuric acid with dust particles (Harris et al., 2012). At Izaña, negative correlations between dust and particles smaller than 10 nm have also been observed (Rodríguez et al., 2009).

Our observations could only be compared with similar studies in the boundary layer, due to the lack of this type of long term studies in mountain observatories. For example, in the Po Valley (Northern Italy), Hamed et al. (2007) observed that temperature, wind speed, solar radiation, SO_2 and O_3 concentrations were on average higher on nucleation days than on non-event days, whereas relative humidity and NO_2 concentration were lower. These conditions are similar to those we observed at Izaña, except for wind speed and ozone (Table 4). At Izaña, a moderate correlation between the concentration of nucleation particles with ozone was observed only in spring, when biogenic emissions tend to increase. Oxidation products of biogenic volatile organic compounds could also take part in the growth processes (Held et al., 2004; Yli-Juuti et al., 2011).

3.4.2 Type Ia versus other type events

The context in which type Ia events occur was compared with that in which the other events (Table 1) occur. For this, the monthly mean value of a set of parameters recorded (from 09:00 to 17:00 GMT) during the different types of events (Ia, Ib, II, III and No event) was compared with the monthly mean value (from 09:00 to 17:00 GMT) for these parameters (Fig. 10). Some features that differentiate the events are: (a) the

Climatology of new particle formation events at Izaña GAW observatory

M. I. García et al.

Title Page

Abstract	Introduction
Conclusions	References
Tables	Figures

|◄ | ►|

◄ | ►

Back | Close

Full Screen / Esc

Printer-friendly Version

Interactive Discussion

highest concentrations of nucleation particles were observed during the different type of banana type events (Ia, Ib and II), when N_{nuc} concentrations are 2 to 3 times higher than during burst (III) episodes (Fig. 10a). (b) SO_2 concentrations during events type I (which last at least 4 h) are higher than during events II (which last 2 to 4 h Fig. 10b). This suggests that the availability of this precursor influence the length of the banana type events. Similarly, SO_2 concentrations are higher during banana type II events, than during burst episodes (III). The availability of this precursor seems to be conditioned by wind speed, observe how wind speed decreases throughout the sequence of episodes no event, III (burst) and banana types II and I (Fig. 10c); a trend opposite to that of SO_2 (Fig. 10b). (c) Except for a few cases, concentrations of NO_x tend to be lower during type I banana events (Fig. 10d). This has also been observed in the continental boundary layer (Boy and Kulmala, 2002; Hamed et al., 2007). (d) During events type I (Ia + Ib) temperature is higher and relative humidity is lower than monthly means values and lower than during burst (III) and no event episodes (Fig. 10e and f). This feature is frequently observed in NPF events (Rodríguez et al., 2005; Hamed et al., 2007; Moorthy et al., 2011; Neitola et al., 2011). (e) Global, UV-A and UV-B radiation during events type I (banana > 4h) tend to be slightly higher than during the other event types (II, III and no event). For events type Ia, this feature is enhanced if mean values are determined just during the formation and growth periods (Fig. 10g, h and i). Other feature of events type Ia is that Global, UV-A and UV-B radiation tend to be higher during the formation step than during the growth step. This link between NPF events and high radiation intensity periods is also a common feature of NPF events (Birmili et al., 2000; Boy and Kulmala, 2002; Dal Maso et al., 2005; Hamed et al., 2007; Qian et al., 2007; Murugavel and Chate, 2009; Yli-Juuti et al., 2009; Manninen et al., 2010; Cheung et al., 2011; Neitola et al., 2011; Salma et al., 2011).

3.5 Year to year variability

Processes that influence the year to year variability of the frequency of each type of episode (Table 1) were studied. For this purpose, the frequency of each type of event

was correlated with the study reactive gases, radiation and meteorological parameters for each season from June 2008 to June 2012. Because of the huge amount of data, here we focus just on the key issues.

The year-to-year variability in the number of banana type events (I+II) exhibited the highest correlation with SO_2. The correlation was higher from autumn to spring (r: 0.7 to 0.92) than in summer (r: 0.05; Fig. 11a–d). This indicates that other processes apart from transport of precursors influence NPF in summertime. In this season, the number of banana type events (I + II) exhibited a significant correlation with direct radiation (Fig. 11g), and an evident negative correlation with diffuse radiation (not shown in plots). Because diffuse radiation is dominated by Saharan dust at Izaña (García et al., 2013), direct radiation is indicative of clean (dust free) conditions. This indicates that the presence of dust may influence the year to year variability in the NPF frequency. This may occur by two processes. First, acting as a condensation sink of the gas phase precursor; see the FR versus dust relationship in Fig. 9A3. Second, reducing the amount of radiation reaching the surface (negative forcing). The number of banana type NPF events (I + II) also exhibited a significant correlation with UV-B radiation during Autumn and Winter (r: +0.9), when they showed their lowest seasonal levels ($\sim 1\,W\,m^{-2}$; Fig. 11i–l). This suggests that UV-B radiation (absorbed by SO_2) may be an important influence parameter in Autumn–Winter, but not in summer because of the persistently high day-to-day levels ($\sim 2\,W\,m^{-2}$).

3.6 Some considerations about the nucleation mode

The determination of the formation and growth rates is usually performed assuming that the size distribution in the nucleation range ($< 25\,nm$) is constituted by a single mode (Boy et al., 2008; Dal Maso et al., 2005; Salma et al., 2011; Yli-Juuti et al., 2009). In many of the type Ia events we analyzed, this hypothesis is supported. However, we detected a significant number of events type Ia in which two nucleation modes were clearly observed. Moreover, the evolution and growth rates of these two modes were in many cases markedly different. Observe in the example shown in Fig. 12 how the nu-

cleation mode 2 (orange arrow) experiences a faster development than the nucleation mode 1 (green arrow).

We then assessed the implication of the occurrences of these 2 nucleation mode events. For this, we performed two types of lognormal fittings in all the type Ia events that occurred from April 2009 to August 2010: 3 lognormal distributions (1 in the nucleation mode, 1 Aitken mode and 1 in the Accumulation mode) and 4 lognormal distributions (2 in the nucleation mode, 1 Aitken mode and 1 in the Accumulation mode). The difference in the total number concentration determined from each fitting to the total number concentrations measured with the SMPS was determined and used as a measure of the error (accuracy) of each fitting. This error was similar in the two fitting when just 1 nucleation mode was present (Fig. 13a), whereas the error was $\sim 40\%$ lower in the case of 2 nucleation mode fitting when the two nucleation modes were present (Fig. 13b). A total of 55 events were studied (April 2009 to August 2010; Fig. 13), the two nucleation mode appeared in 47 % of these events (Fig. 13a).

Finally, in a selection of four type Ia events, the growth rates was calculated with 3 different techniques: (i) directly with the SMPS data (as for data of Figs. 7–9), (ii) after performing a fitting to 3 lognormal distributions (1 nucleation, 1 Aitken and 1 Accumulation mode), and (iii) after performing a fitting to 4 lognormal distributions (2 nucleation, 1 Aitken and 1 Accumulation mode). GR obtained from the "1 lognormal mode nucleation fitting" are higher than those obtained directly from the SMPS data (Table 5). Differences in the GR when comparing different techniques were also described by Yli-Juuti et al. (2009). When considering the two nucleation mode fittings, in some cases the GR of mode 1 is higher than that of the mode 2, and the opposite. This illustrates how the two nucleation modes may have markedly different evolution.

4   Summary and conclusions

A climatology of NPF events at Izaña mountain, the only Global Atmospheric Watch observatory located in the North Atlantic free troposphere, is presented here. A total

Climatology of new particle formation events at Izaña GAW observatory

M. I. García et al.

Title Page

Abstract | Introduction

Conclusions | References

Tables | Figures

◄ | ►

◄ | ►

Back | Close

Full Screen / Esc

Printer-friendly Version

Interactive Discussion

of 1178 days were studied from June 2008 to June 2012. NPF was observed during $\sim 30\%$ of the days. There is a clearly marked NPF season (May to August), when these events account for 50 to 60 % of the days/month. In contrast, burst of nucleation particles (not followed by particle growth) occurs throughout the year. Monthly mean values of the formation and growth rates exhibit higher values during the NPF season (0.50–0.95 cm^{-3} s^{-1} and 0.48–0.58 nm h^{-1}, respectively) than during other periods. The overall data analysis shows that sulphur dioxide and UV radiation have an influence on NPF, both during the formation and growth steps. Moreover, the presence of Saharan dust in the free troposphere is associated with a decrease in the formation rates of new particles. In the analysis of the year-to-year variability, mean sulphur dioxide concentration (within the range 60 to 300 ppt) was the parameter that exhibited the highest correlation with the frequency of NPF episodes.

We have had difficulties in comparing our results with those obtained from other observatories, due to the deficit of long term NPF studies in free troposphere sites. The formation and growth rates we observed are close to those observed in Mauna Loa (Hawaii). However, the formation rates at Izaña are significantly lower than those observed in mounts located in continental regions, e.g.: Jungfraujoch and Puy de Dôme in Europe, Pyramide and Mukteshwar in Asia, Lemmon and Rocky Mountains in North America and Dome C in Antarctica.

We observed that in 47 % of the NPF events two nucleation modes were clearly present. The calculation of the formation and growth rates has usually been performed (including this study) assuming that the nucleation mode is constituted by just one mode. We observed that these two nucleation modes may evolve at different rates,and the growth rates of each mode are different to the growth rate if just one nucleation mode is assumed. This has implications for the parameterization of NPF events. Further investigations are necessary.

Climatology of new particle formation events at Izaña GAW observatory

M. I. García et al.

Title Page

Abstract | Introduction

Conclusions | References

Tables | Figures

⏮ | ⏭

◀ | ▶

Back | Close

Full Screen / Esc

Printer-friendly Version

Interactive Discussion

References

Asmi, A., Collaud Coen, M., Ogren, J. A., Andrews, E., Sheridan, P., Jefferson, A., Weingartner, E., Baltensperger, U., Bukowiecki, N., Lihavainen, H., Kivekäs, N., Asmi, E., Aalto, P. P., Kulmala, M., Wiedensohler, A., Birmili, W., Hamed, A., O'Dowd, C., G Jennings, S., Weller, R., Flentje, H., Fjaeraa, A. M., Fiebig, M., Myhre, C. L., Hallar, A. G., Swietlicki, E., Kristensson, A., and Laj, P.: Aerosol decadal trends – Part 2: In-situ aerosol particle number concentrations at GAW and ACTRIS stations, Atmos. Chem. Phys., 13, 895–916, doi:10.5194/acp-13-895-2013, 2013. 24129

Birmili, W. and Wiedensohler, A.: New particle formation in the continental boundary layer: Meteorological and gas phase parameter influence, Geophys. Res. Lett., 27, 3325, doi:10.1029/1999GL011221,2000. 24130, 24142

Boulon, J., Sellegri, K., Venzac, H., Picard, D., Weingartner, E., Wehrle, G., Collaud Coen, M., Bütikofer, R., Flückiger, E., Baltensperger, U., and Laj, P.: New particle formation and ultrafine charged aerosol climatology at a high altitude site in the Alps (Jungfraujoch, 3580 m a.s.l., Switzerland), Atmos. Chem. Phys., 10, 9333–9349, doi:10.5194/acp-10-9333-2010, 2010. 24138

Boy, M. and Kulmala, M.: Nucleation events in the continental boundary layer: Influence of physical and meteorological parameters, Atmos. Chem. Phys., 2, 1–16, doi:10.5194/acp-2-1-2002, 2002. 24142

Boy, M., Karl, T., Turnipseed, A., Mauldin, R. L., Kosciuch, E., Greenberg, J., Rathbone, J., Smith, J., Held, A., Barsanti, K., Wehner, B., Bauer, S., Wiedensohler, A., Bonn, B., Kulmala, M., and Guenther, A.: New particle formation in the Front Range of the Colorado

Climatology of new particle formation events at Izaña GAW observatory

M. I. García et al.

Title Page

Abstract	Introduction
Conclusions	References
Tables	Figures

◄ | ►

◄ | ►

Back | Close

Full Screen / Esc

Printer-friendly Version

Interactive Discussion

Rocky Mountains, Atmos. Chem. Phys., 8, 1577–1590, doi:10.5194/acp-8-1577-2008, 2008. 24135, 24143

Cheung, H. C., Morawska, L., and Ristovski, Z. D.: Observation of new particle formation in subtropical urban environment, Atmos. Chem. Phys., 11, 3823–3833, doi:10.5194/acp-11-3823-2011, 2011. 24142

Dal Maso, M., Kulmala M., Riipinen, I., Wagner, R., Hussein, T., Aalto, P. P., and Lehtinen, K. E. J.: Formation and growth of freshatmospheric aerosols: eight years of aerosol size distribution data from SMEAR II, Hyytiälä, Finland, Boreal Environ. Res., 10, 323–336, 2005. 24130, 24133, 24135, 24138, 24142, 24143

Fiedler, V., Dal Maso, M., Boy, M., Aufmhoff, H., Hoffmann, J., Schuck, T., Birmili, W., Hanke, M., Uecker, J., Arnold, F., and Kulmala, M.: The contribution of sulphuric acid to atmospheric particle formation and growth: a comparison between boundary layers in Northern and Central Europe, Atmos. Chem. Phys., 5, 1773–1785, doi:10.5194/acp-5-1773-2005, 2005. 24141

García, R. D.: Aplicación de modelos de transferencia radiativa para el control operativo del programa BSRN (Base-line Surface Radiation Network) del Centro de Investigación Atmosférica de Izaña, PhD Thesis, Univ. of Valladolid at Spain, December 2011. 24133

García, R. D., García, O. E., Cuevas, E., Cachorro, V. E., Romero-Campos, P.M., Ramos, R., and Frutos, A. M.: Solar irradiance measurements compared to simulations at the BSRN Izaña station. Mineral dust radiative forcing and efficiency study, J. Geophys. Res., submitted, 2013. 24143

Gómez-Moreno, F. J., Alonso, E., Artiñano, B., Juncal Bello, V., Piñeiro Iglesias, M., López Mahía, P., Pérez, N., Pey, J., Alastuey, A., de la Morena, B. A., García, M. I., Rodríguez, S., Sorribas, M., Titos, G., Lyamani, H., and Alados-Arboledas, L.: The Spanish network on environmental DMAs: the 2012 SMPS+UFP intercomparison campaign and study on particle losses in dryers, European Aerosol Conference, Prague, 1–6 September 2013. 24131

Hamed, A., Joutsensaari, J., Mikkonen, S., Sogacheva, L., Dal Maso, M., Kulmala, M., Cavalli, F., Fuzzi, S., Facchini, M. C., Decesari, S., Mircea, M., Lehtinen, K. E. J., and Laaksonen, A.: Nucleation and growth of new particles in Po Valley, Italy, Atmos. Chem. Phys., 7, 355–376, doi:10.5194/acp-7-355-2007, 2007. 24130, 24138, 24141, 24142

Harris, E., Sinha, B., Foley, S., Crowley, J. N., Borrmann, S., and Hoppe, P.: Sulfur isotope fractionation during heterogeneous oxidation of SO_2 on mineral dust, Atmos. Chem. Phys., 12, 4867–4884, doi:10.5194/acp-12-4867-2012, 2012. 24141

Title Page

Abstract | Introduction

Conclusions | References

Tables | Figures

|◄ | ►|

◄ | ►

Back | Close

Full Screen / Esc

Printer-friendly Version

Interactive Discussion

Held, A., Nowak, A., Birmili, W., Wiedensohler, A., Forkel, R., and Klemm, O.: Observations of particle formation and growth in a mountainous forest region in central Europe, J. Geophys. Res., 109, 1–9, doi:10.1029/2004JD005346, 2004. 24141

Hinds, W. C.: Aerosol Technology, Properties behaviour and measurements of airborne particles, Wiley-Interscience. John Wiley & Sons, Inc. Canada, 1999. 24132

Hussein, T., Dal Maso, M., Petäjä, T., Koponen, I. K., Paatero, P., Aalto, P. P., Hämeri, K., and Kulmala, M.: Evaluation of an automatic algorithm for fitting the particle number size distribution, Boreal Environ. Res., 10, 337–355, 2005.

IPCC: Climate Change 2007, The Physical Science Basis, Contribution of Working Group I to the Fourth Assessment Report of the Intergovernmental Panel on Climate Change, Cambridge University Press, New York, 2007.

Järvinen, E., Virkkula, A., Nieminen, T., Aalto, P. P., Asmi, E., Lanconelli, C., Busetto, M., Lupi, A., Schioppo, R., Vitale, V., Mazzola, M., Petäjä, T., Kerminen, V.-M., and Kulmala, M.: Seasonal cycle and modal structure of particle number size distribution at Dome C, Antarctica, Atmos. Chem. Phys., 13, 7473–7487, doi:10.5194/acp-13-7473-2013, 2013. 24135, 24138

Kleissl, J., Honrath, R. E., Dziobak, M. P., Tanner, D., Val Martín, M., Owen, R. C., and Helmig, D.: Occurrence of upslope flows at the Pico mountaintop observatory: A case study of orographic flows on a small, volcanic island, J. Geophys. Res., 112, D10S35, doi:10.1029/2006JD007565, 2007 24136

Kulmala, M.: How Particles Nucleate and Grow, Science, 302, 100–1001, 2003. 24128, 24129

Kulmala, M., Vehkamäki, H., Petäjä, T., Dal Maso, M., Lauri, A., Kerminen, V.-M., Birmili, W., and McMurry, P. H.: Formation and growth rates of ultrafine atmospheric particles: a review of observations, J. Aerosol Science, 35, 143–176, doi:10.1016/j.jaerosci.2003.10.003, 2004. 24129, 24134

Kulmala, M., Lehtinen, K. E. J., and Laaksonen, A.: Cluster activation theory as an explanation of the linear dependence between formation rate of 3 nm particles and sulphuric acid concentration, Atmos. Chem. Phys., 6, 787–793, doi:10.5194/acp-6-787-2006, 2006. 24129

Kulmala, M. and Kerminen, V. M.: On the formation and growth of Atmospheric nanoparticles, Atmos. Res., 90, 132–150, 2008. 24129

Laaksonen, A., Kulmala, M., O'Dowd, C. D., Joutsensaari, J., Vaattovaara, P., Mikkonen, S., Lehtinen, K. E. J., Sogacheva, L., Dal Maso, M., Aalto, P., Petäjä, T., Sogachev, A., Yoon, Y. J., Lihavainen, H., Nilsson, D., Facchini, M. C., Cavalli, F., Fuzzi, S., Hoffmann, T., Arnold, F., Hanke, M., Sellegri, K., Umann, B., Junkermann, W., Coe, H., Allan, J. D., Alfarra, M.

R., Worsnop, D. R., Riekkola, M.-L., Hyötyläinen, T., and Viisanen, Y.: The role of VOC oxidation products in continental new particle formation, Atmos. Chem. Phys., 8, 2657–2665, doi:10.5194/acp-8-2657-2008, 2008. 24129, 24141

Manninen, H. E., Nieminen, T., Asmi, E., Gagné, S., Häkkinen, S., Lehtipalo, K., Aalto, P., Vana, M., Mirme, A., Mirme, S., Hõrrak, U., Plass-Dülmer, C., Stange, G., Kiss, G., Hoffer, A., Törö, N., Moerman, M., Henzing, B., de Leeuw, G., Brinkenberg, M., Kouvarakis, G. N., Bougiatioti, A., Mihalopoulos, N., O'Dowd, C., Ceburnis, D., Arneth, A., Svenningsson, B., Swietlicki, E., Tarozzi, L., Decesari, S., Facchini, M. C., Birmili, W., Sonntag, A., Wiedensohler, A., Boulon, J., Sellegri, K., Laj, P., Gysel, M., Bukowiecki, N., Weingartner, E., Wehrle, G., Laaksonen, A., Hamed, A., Joutsensaari, J., Petäjä, T., Kerminen, V.-M., and Kulmala, M.: EUCAARI ion spectrometer measurements at 12 European sites – analysis of new particle formation events, Atmos. Chem. Phys., 10, 7907–7927, doi:10.5194/acp-10-7907-2010, 2010. 24137, 24138, 24142

McFiggans, G., Artaxo, P., Baltensperger, U., Coe, H., Facchini, M. C., Feingold, G., Fuzzi, S., Gysel, M., Laaksonen, A., Lohmann, U., Mentel, T. F., Murphy, D. M., O'Dowd, C. D., Snider, J. R., and Weingartner, E.: The effect of physical and chemical aerosol properties on warm cloud droplet activation, Atmos. Chem. Phys., 6, 2593-2649, doi:10.5194/acp-6-2593-2006, 2006. 24129

Moorthy, K. K., Sreekanth, V., Chaubey, J. P., Gogoi, M. M., Babu, S. S., Kompalli, S. K., Bagare, S. P., Bhatt, B. C., Gaur, V. K., Prabhu, T. P., and Singh, N. S.: Fine and ultrafine particles at a near-free tropospheric environment over the high-altitude station Hanle in the Trans-Himalaya: New particle formation and size distribution, J. Geophys. Res., 116, 1–12, doi:10.1029/2011JD016343, 2011. 24142

Murugavel, P. and Chate, D.: Generation and growth of aerosols over Pune, India, Atmos. Environ., 43, 820–828, doi:10.1016/j.atmosenv.2008.10.051, 2009. 24142

Neitola, K., Asmi, E., Komppula, M., Hyvärinen, A.-P., Raatikainen, T., Panwar, T. S., Sharma, V. P., and Lihavainen, H.: New particle formation infrequently observed in Himalayan foothills – why?, Atmos. Chem. Phys., 11, 8447–8458, doi:10.5194/acp-11-8447-2011, 2011. 24137, 24138, 24142

Nishita, C., Osada, K., Kido, M., Matsunaga, K., and Iwasaka, Y.: Nucleation mode particles in upslope valley winds at Mount Norikura, Japan: Implications for the vertical extent of new particle formation events in the lower troposphere, J. Geophys. Res., 113, D06202, doi:10.1029/2007JD009302, 2008.

Title Page

Abstract | Introduction

Conclusions | References

Tables | Figures

◁◁ | ▷▷

◁ | ▷

Back | Close

Full Screen / Esc

Printer-friendly Version

Interactive Discussion

Parrish, D. D. and Fehsenfeld, F. C.: Methods for gas-phase measurements of ozone, ozone precursors and aerosol precursors, Atmos. Environ., 34, 1921–1957, 2000. 24132

Qian, S., Sakurai, H., and McMurry, P. H.: Characteristics of regional nucleation events in urban East St. Louis, Atmos. Environ., 41, 4119–4127, doi:10.1016/j.atmosenv.2007.01.011, 2007. 24142

Rodríguez, S., Van Dingenen, R., Putaud, J. P., Martins-Dos Santos, S., and Roselli, D.: Nucleation and growth of new particles in the rural atmosphere of Northern Italy – Relationship to air quality monitoring, Atmos. Environ., 39, 6734–6746, 2005. 24138, 24142

Rodríguez, S., González, Y., Cuevas, E., Ramos, R., Romero, P. M., Abreu-Afonso, J., and Redondas, A.: Atmospheric nanoparticle observations in the low free troposphere during upward orographic flows at Izaña Mountain Observatory, Atmos. Chem. Phys., 9, 6319–6335, doi:10.5194/acp-9-6319-2009, 2009. 24130, 24136, 24137, 24141

Rodríguez, S., Alastuey, A., Alonso-Pérez, S., Querol, X., Cuevas, E., Abreu-Afonso, J., Viana, M., Pérez, N., Pandolfi, M., and de la Rosa, J.: Transport of desert dust mixed with North African industrial pollutants in the subtropical Saharan Air Layer, Atmos. Chem. Phys., 11, 6663–6685, doi:10.5194/acp-11-6663-2011, 2011. 24132

Salma, I., Borsós, T., Weidinger, T., Aalto, P., Hussein, T., Dal Maso, M., and Kulmala, M.: Production, growth and properties of ultrafine atmospheric aerosol particles in an urban environment, Atmos. Chem. Phys., 11, 1339–1353, doi:10.5194/acp-11-1339-2011, 2011. 24135, 24142, 24143

Shaw, G. E.: Aerosols at a mountaintop observatory in Arizona, J. Geophys. Res., 112, D07206, doi:10.1029/2005JD006893, 2007.

Steinbacher, M., Zellweger, C., Schwarzenbach, B., Bugmann, S., Buchmann, B., Ordóñez, C., Prevot, A. S. H., and Hueglin, C., Nitrogen oxide measurements at rural sites in Switzerland: Bias of conventional measurement techniques, J. Geophys. Res., 112, D11307, doi:10.1029/2006JD007971, 2007. 24132

Venzac, H., Sellegri, K., Laj, P., Villani, P., Bonasoni, P., Marioni, A., Cristofanelli, P., Calzolari, F., Fuzzi, S., Decesari, S., Facchini, M.-C., Vuillermoz, E., and Verza, G.-P.: High frequency new particle formation in the Himalayas, P. Natl. Acad. Sci. USA, 105, 15666–15671, 2008. 24130, 24137, 24139

Venzac, H., Sellegri, K., Villani, P., Picard, D., and Laj, P.: Seasonal variation of aerosol size distributions in the free troposphere and residual layer at the puy de Dôme station, France, Atmos. Chem. Phys., 9, 1465–1478, doi:10.5194/acp-9-1465-2009, 2009.

Title Page

Abstract | Introduction

Conclusions | References

Tables | Figures

Back | Close

Full Screen / Esc

Printer-friendly Version

Interactive Discussion

Weber, J. R., McMurry, P. H., Eisele, F. L., and Tanner, D. J.: Measurements of expected nucleation precursors species and 3–500 nm diameter particles at Mauna Loa, Hawaii, J. Atmos. Sci., 52, 2242–2257, 1995. 24130, 24136

Weber, J. R., McMurry, P. H., Mauldin III, R. L., Tanner, D. J., Eisele, F. L., Clarke, A. D., and Kapustin, V. N.: New particle formation in the remote troposphere: a comparison of observations at various sites, Geophys. Res. Lett., 26, 307–310, 1999. 24136

Yli-Juuti, T., Riipinen, I., Aalto, P. P., Nieminen, T., Maenhaut, W., Janssens, I. A., Claeys, M., Salma, I., Ocskay, R., Hoffer, A., Imre, K., and Kulmala, M.: Characteristics of new particle formation events and cluster ions at K-puszta, Hungary, Boreal Environ. Res., 14, 683–698, 2009. 24134, 24135, 24142, 24143, 24144

Yli-Juuti, T., Nieminen, T., Hirsikko, A., Aalto, P. P., Asmi, E., Hõrrak, U., Manninen, H. E., Patokoski, J., Dal Maso, M., Petäjä, T., Rinne, J., Kulmala, M., and Riipinen, I.: Growth rates of nucleation mode particles in Hyytiälä during 2003–2009: variation with particle size, season, data analysis method and ambient conditions, Atmos. Chem. Phys., 11, 12865-12886, doi:10.5194/acp-11-12865-2011, 2011. 24141

Title Page

Abstract | Introduction

Conclusions | References

Tables | Figures

◄ | ►

◄ | ►

Back | Close

Full Screen / Esc

Printer-friendly Version

Interactive Discussion

Table 1. Type of events considered in this study. FR: formation rates. GR: Growth rates.

Type	Criteria
Class Ia (banana type)	A new mode with growing mean diameter under 25 nm is observed. The growth is observed during at least 4 h. FR and GR can be calculated.
Class Ib (banana type)	A new mode with growing mean diameter under 25 nm is observed. The growth is observed during at least 4 h, but FR and GR could not be calculated.
Class II (short banana type)	A new mode with growing mean diameter under 25 nm is observed. The growth period lasts from 2 to 4 h.
Class III (apple/burst)	A new mode with growing mean diameter under 25 nm is observed. The growth period is lower than 2 h.
Non-Event	No new particle mode with mean diameter under 25 nm is observed.
Undefined	Event is not clearly observed.
Bad Data	Missing or invalid data.

Table 2. Total number and percentage of events observed from June 2008 to June 2012.

Event type	Number of events	%
Class Ia	109	9.3
Class Ib	26	2.2
Class II	227	19.3
Class III	101	8.6
Non- Event	514	43.6
Undefined	50	4.2
Bad Data	151	12.8
Total days	1178	100.0

Table 3. Values of Formation Rates and Growth Rates observed in this and in other studies at mountain sites. Super index indicate the reference.

Mount/Observatory	FR, $cm^{-3} s^{-1}$	size range	GR, $nm\,h^{-1}$	size range	Region	Altitude, m a.s.l
Izaña	0.54 ± 0.57[1]	10–25 nm	0.43 ± 0.21[1]	10–25 nm	Atlantic Ocean	2400
Mauna Loa	0.50 ± 0.57[2a]	3–10 nm	$0.40 \pm$ N/A[2b]	> 10 nm	Pacific Ocean	3400
Jungfraujoch	$0.90 \pm$ N/A[3a]	> 1 nm	$6.00 \pm$ N/A[3b]	7–20 nm	Europe	3580
Puy de Dôme			5.00 ± 3.50[4]	7–20 nm	Europe	1465
Pyramide	$0.17 \pm$ N/A[5]	10–20 nm	1.80 ± 0.70[5]	10–20 nm	Asia, Everest	5079
Mukteshwar	$0.40 \pm$ N/A[6]	15–20 nm	$2.43 \pm$ N/A[6]	15–20 nm	Asia, Himalaya	2180
Norikura			$2.85 \pm$ N/A[7]	10–20 nm	Asia, Japan	2770
Mt. Lemmon			$16.50 \pm$ N/A[8]	10–18 nm	North America	2790
Rocky Mountains			$3.96 \pm$ N/A[9]	1–15 nm	North America	2900
Dome C	$0.023 \pm$ N/A[10]	10–25 nm	$2.50 \pm$ N/A[10]	10–25 nm	Antarctica	3200

[1] this study
[2a] Weber et al. (1999)
[2b] Weber et al. (1995)
[3a] Manninen et al. (2010)
[3b] Boulon et al. (2010), Manninen et al. (2010)
[4] Venzac (2008), Manninen et al. (2010)
[5] Venzac et al. (2008)
[6] Neitola et al. (2011)
[7] Nishita et al. (2008)
[8] Shaw (2007)
[9] Boy et al. (2008)
[10] Järvinen et al. (2013)

Table 4. Mean values of a set of parameters in three different periods: (a) from 08:00 to 20:00 GMT during the whole study period "All period", (b) during the formation of the nucleation mode particles step (F) in the NPF episodes, (c) during the particle growth step (G) in the NPF episodes. Ratios of the mean "F step to all period" data, and of "G step to all period". Ratios ≥ 1.5 are highlighted.

Parameter	(a) All period, mean	(b) F step, mean	(c) G step, mean	F step, ratio	G step, ratio
Ozone (ppb)	44.4	42.3	42.9	1.0	1.0
SO_2 (ppt)	105.3	238.3	233.7	2.3	2.2
NO_x (ppt)	252.4	204.0	196.7	0.8	0.8
Global ($W\,m^{-2}$)	560.8	881.5	833.1	1.6	1.5
Difusse ($W\,m^{-2}$)	693.5	940.4	884.0	1.4	1.3
Direct ($W\,m^{-2}$)	110.0	128.4	129.5	1.2	1.2
UV-B ($W\,m^{-2}$)	0.9	1.7	1.6	1.9	1.8
UV-A ($W\,m^{-2}$)	34.7	56.3	53.4	1.6	1.5
T (°C)	13.1	18.4	18.1	1.4	1.4
Relative Humidity (%)	37.5	29.2	32.0	0.8	0.9
Water Vapour ($g\,cm^{-3}$)	2.9	2.8	3.1	1.0	1.1
Wind speed ($m\,s^{-1}$)	7.8	4.7	4.7	0.6	0.6
Wind X-Component ($m\,s^{-1}$)	2.1	0.8	1.1	0.4	0.5
Wind Y-Component ($m\,s^{-1}$)	−3.2	0.0	−0.4	0.1	0.1
Vertical Wind ($m\,s^{-1}$)	1.5	2.7	3.2	1.8	2.2

Table 5. Mean values of growth rates during four type Ia determined with 3 methods: (1) SMPS data, (2) fitting to 3 lognormal mode with 1 nucleation mode, (3) fitting to 4 lognormal mode with 2 nucleation mode.

Method Day	GR, $\mathrm{nm\,h^{-1}}$ SMPS data	GR, $\mathrm{nm\,h^{-1}}$ 1 nuc. mode fitting	GR, $\mathrm{nm\,h^{-1}}$ 2 nuc. mode fitting (nuc. mode 1)	GR, $\mathrm{nm\,h^{-1}}$ 2 nuc. mode fitting (nuc. mode 2)
30 May 2009	0.98	1.40	0.27	0.58
5 Jul 2009	0.46	1.74	1.01	0.55
16 Aug 2010	0.39	1.40	0.83	0.56
20 Aug 2010	0.90	3.44	0.59	1.59
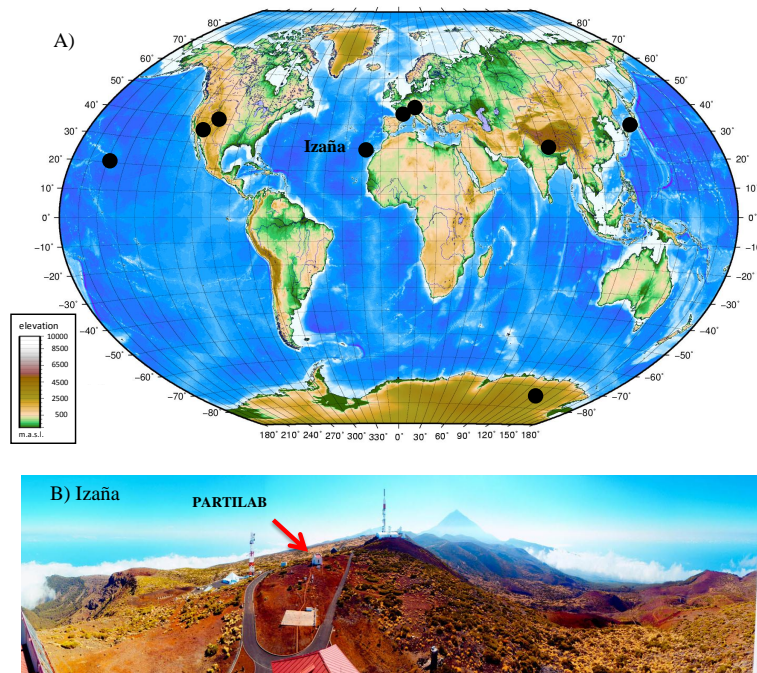
Fig. 1. (A) Global map highlighting the location of Izaña and of other mountain observatories where studies on NPF have been performed. From West to East: Mauna Loa – Hawaii (3400 m a.s.l.; Weber et al., 1995, 1999), Mt. Lemmon – Arizona (2700 m a.s.l.; Shaw et al., 2007), Rocky Mountains – Colorado (2900 m a.s.l.; Boy et al., 2008), Izaña – Tenerife (2367 m a.s.l.; this study), Puy de Dôme – France (1465 m a.s.l.; Venzac, 2009), Jungfraujoch – Swiss Alps (3580 m a.s.l.; Boulon et al., 2010), Pyramide – Nepal (5079 m a.s.l.; Venzac et al., 2008), Norikura – Japan (2770 m a.s.l.; Nishita et al., 2008) and Dome C – Antarctica (3200 m a.s.l.; Järvinen et al., 2013). **(B)** View of the PARTILAB (particles laboratory) from the Izaña observatory main building.
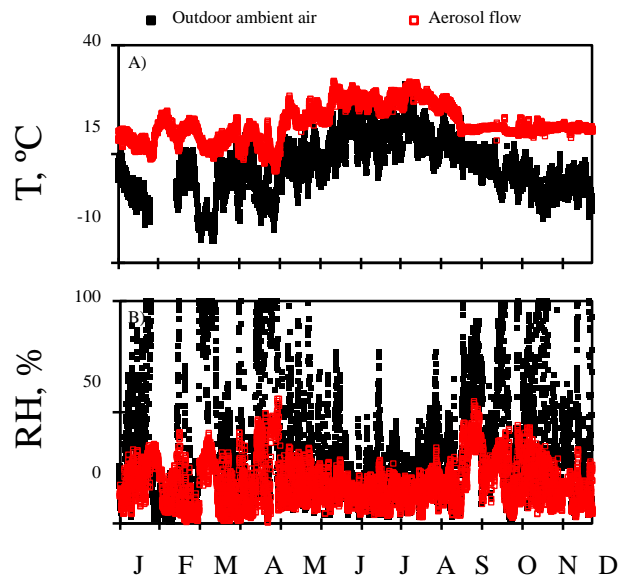
Fig. 2. Hourly mean values of temperature and relative humidity in the outdoor ambient air and in the aerosol flow of the SMPS during 2011.
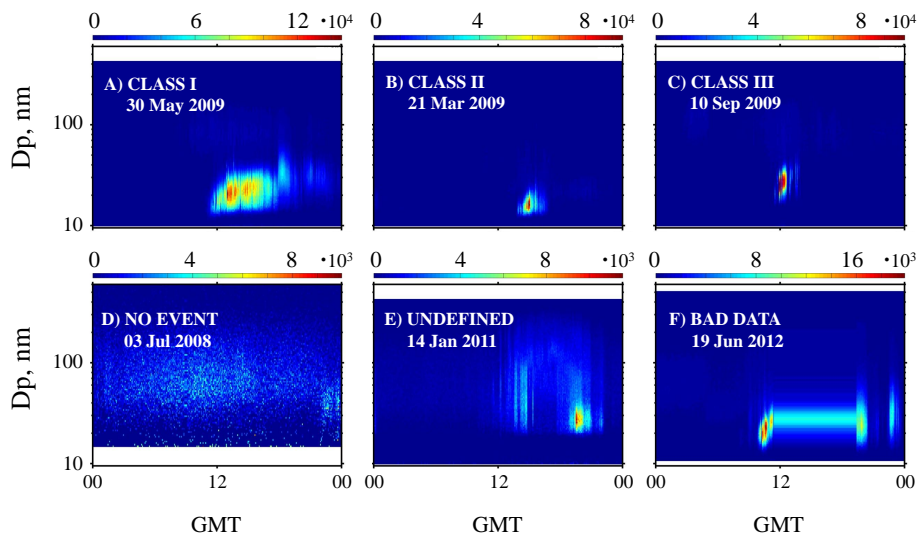
Fig. 3. Examples of type of events and cases identified in the data analysis.
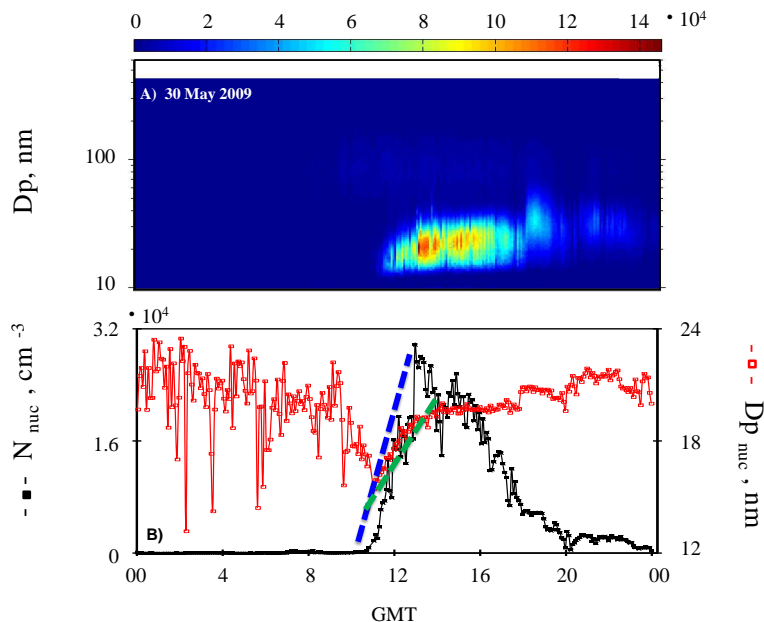
Fig. 4. Example of type Ia event. Time evolution of the particle size distribution **(A)**, of the number of nucleation particles and of the geometric mean diameter for the nucleation mode **(B)**. Lines illustrate the fitting that are performed for determining the formation and growth rates.
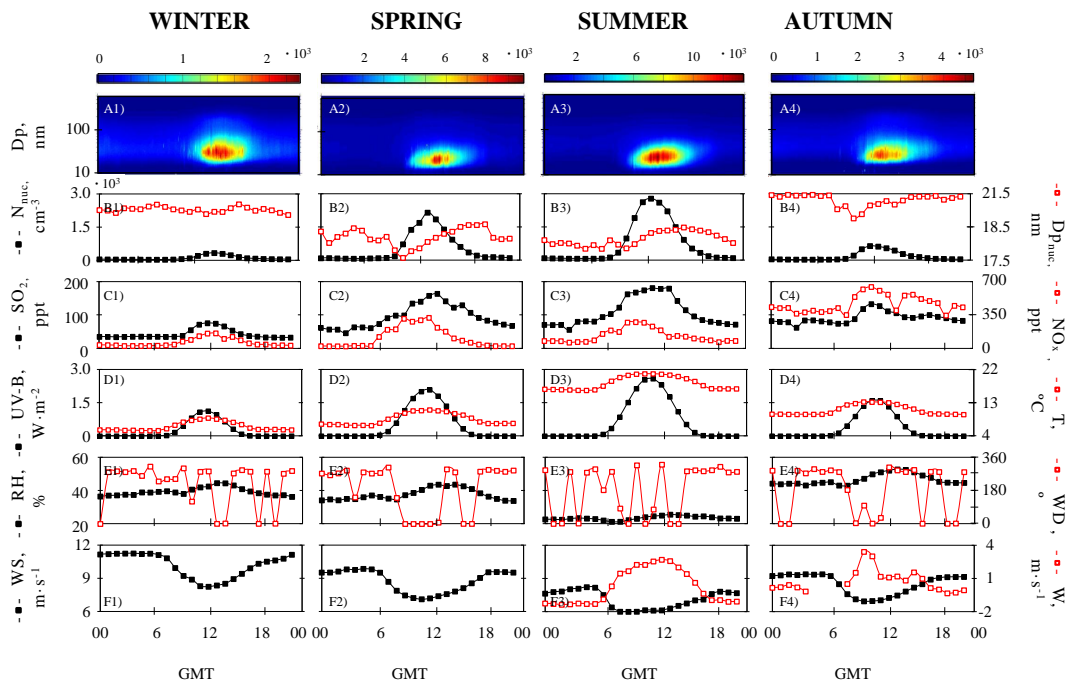
Fig. 5. Daily evolution (hourly mean values) per season of: **(A)** dN/dlog$D$, **(B)** nucleation mode particle concentrations (N_{nuc}) and the geometric mean diameter (Dp$_{nuc}$), **(C)** SO$_2$ and NO$_x$, **(D)** UV-B and temperature (T), **(E)** relative humidity (RH) and wind direction (WD), **(F)** horizontal wind (WS) and vertical (W) wind.
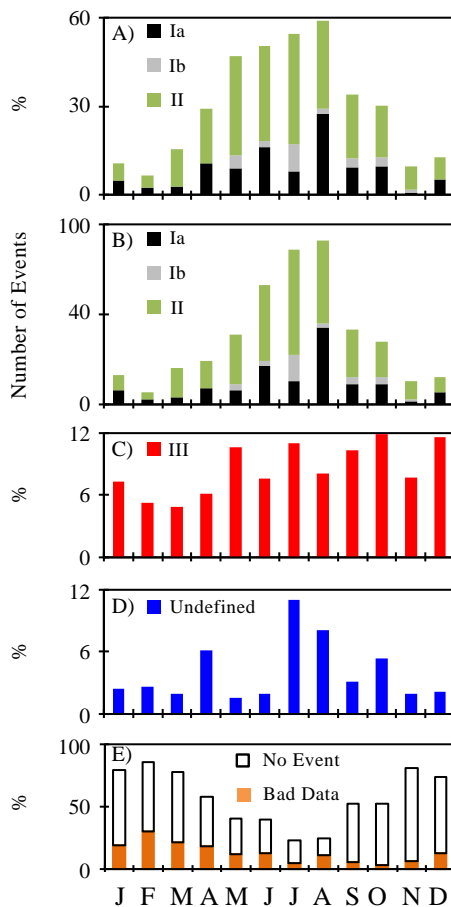
Fig. 6. Monthly distribution of the seven types of events considered in this study.
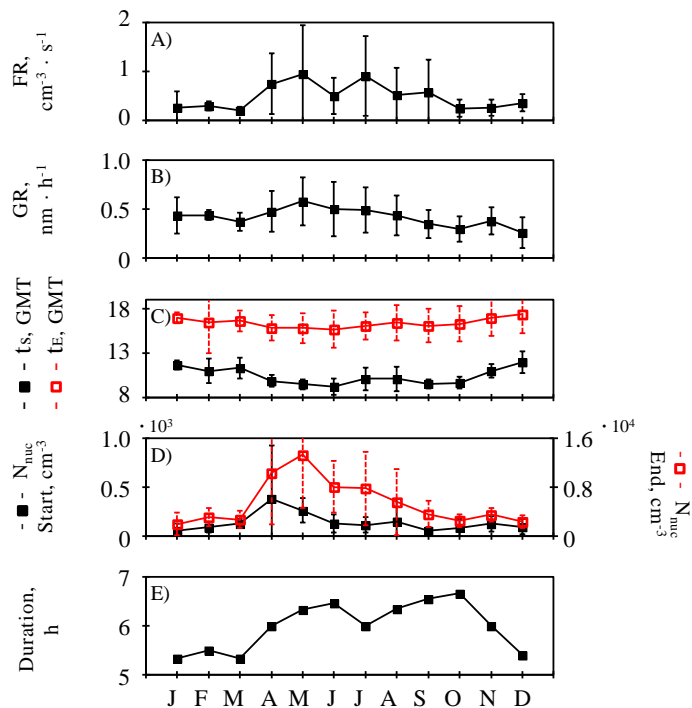
Fig. 7. Monthly mean ± standard deviation values, during la episodes, of: **(A)** Formation rates (FR), **(B)** Growth rates (GR), **(C)** start (t_S) and end (t_E) time of the events, **(D)** nucleation particle concentration at the start (N_{nuc} Start) and burst peak of the event (N_{nuc} End), **(E)** duration of events.

Title Page

Abstract | Introduction

Conclusions | References

Tables | Figures

|◀ | ▶|

◀ | ▶

Back | Close

Full Screen / Esc

Printer-friendly Version

Interactive Discussion
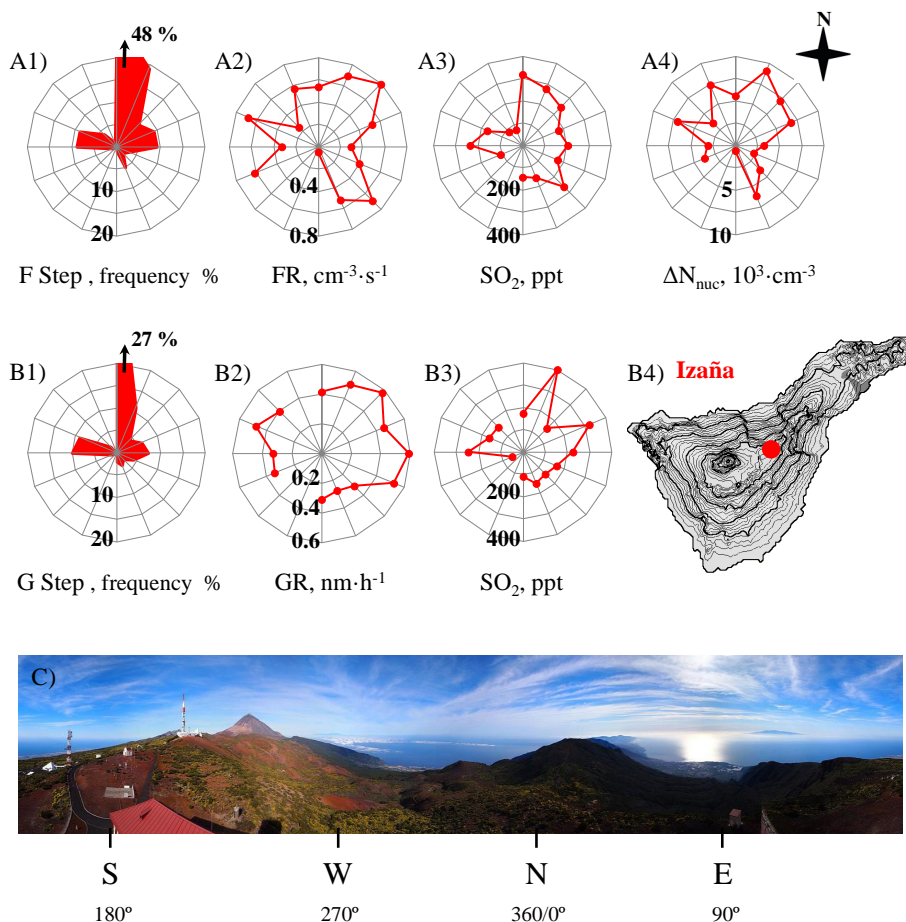
Fig. 8. Wind rose for formation step parameters (**A** frequency, formation rates, SO_2 and nucleation particles concentration) and for growth step parameters (**B** frequency, growth rates and SO_2 concentration). Topographic map of Tenerife **(B4)**. 360° view from Izaña observatory **(C)**.
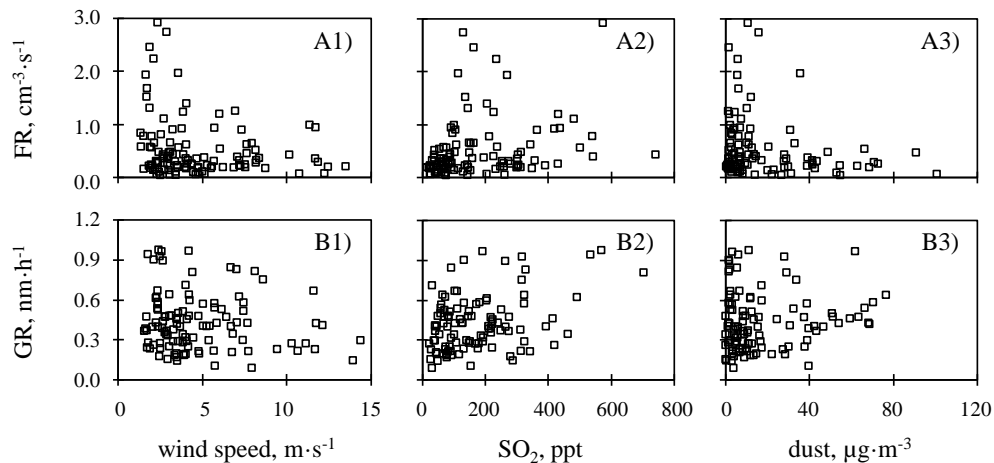
Fig. 9. Scatter plots of the formation rates (FR) and growth rates (GR) versus wind speed, SO_2 and dust concentration at Izaña during the NPF events (type Ia) occurring from June 2008 to June 2012.
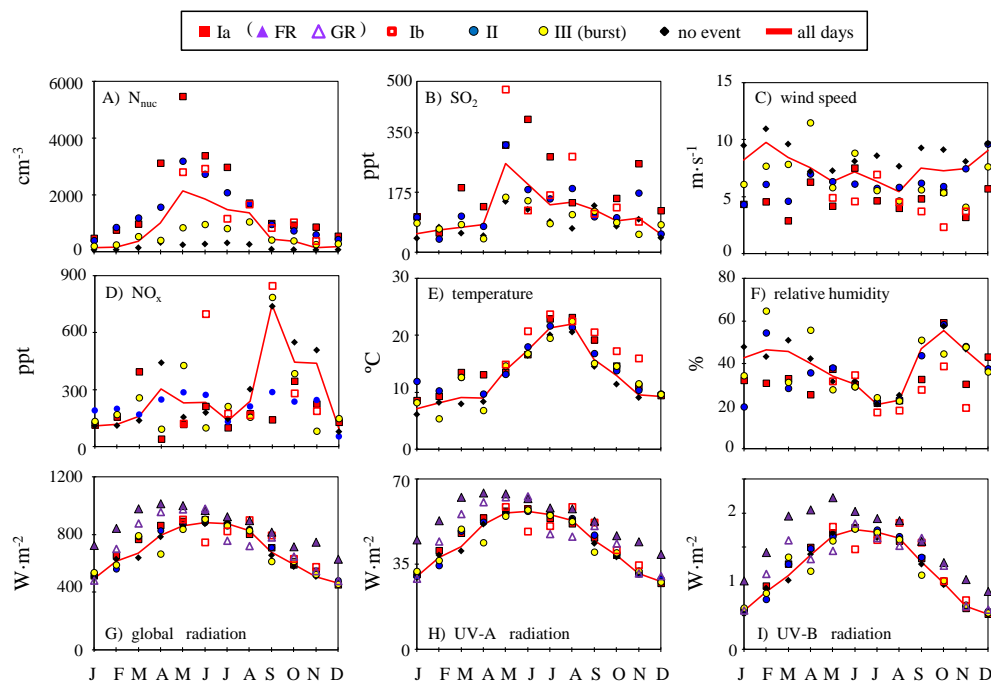
Fig. 10. Monthly mean values (calculated with hourly mean values from 09:00 to 17:00 GMT) of a set of parameters during days in which episodes type Ia, Ib, II, III and No event were registered. Mean values with all days of the months is also included.
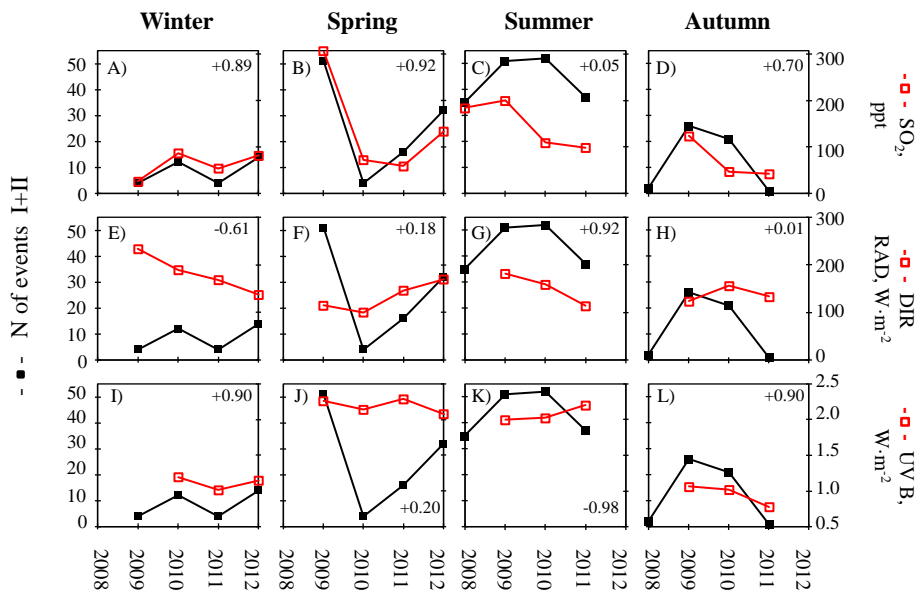
Fig. 11. Number of banana type events (I + II) and mean values (09:00 to 17:00 GMT) of SO_2 and UV-B radiation per season for the period June 2008–June 2012 at Izaña. Winter (Jan-Mar), Spring (April–June), Summer (July–Septmeber) and Autumn (October–December).
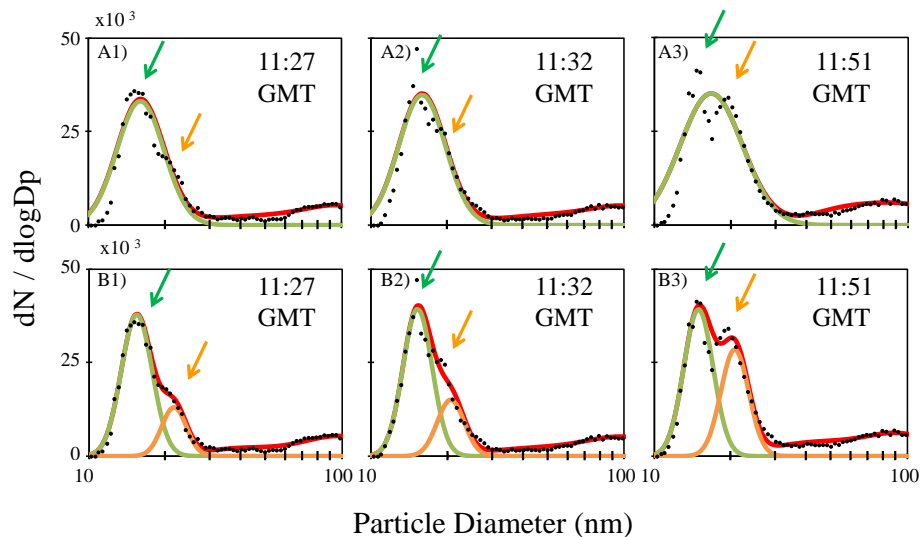
Fig. 12. Example of a banana type Ia event (30 May 2009) in which two nucleation modes were observed (highlighted with green and orange arrows). **(A)** Fitting to 2 lognormal distributions with one nucleation mode (green line). **(B)** Fitting to 3 lognormal distributions with two nucleation modes (green and orange lines). Black dots represent measured data; red line represents the sum of the all the fitted modes.
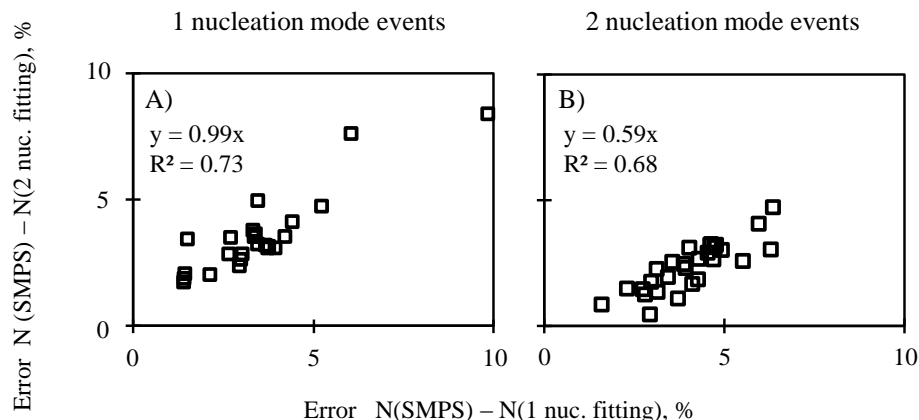
Fig. 13. Difference between the particle number concentrations obtained with 4 lognormal fittings and the number concentrations measured with the SMPS versus the difference between the particle number concentrations obtained with 3 lognormal fittings and the number concentrations measured with the SMPS.